INSTABILITIES AND STRUCTURE FORMATION IN LASER PROCESSING

D. BÄUERLE, E. ARENHOLZ, N. ARNOLD, J. HEITZ, and P.B. KARGL
Angewandte Physik, Johannes-Kepler-Universität Linz, A-4040 Linz, Austria,
dieter.baeuerle@jk.uni-linz.ac.at

ABSTRACT

This paper gives an overview on different types of instabilities and
structure formation in various fields of laser processing. Among the examples
discussed in detail are non-coherent structures observed in laser-induced
chemical vapor deposition (LCVD), in laser-induced surface modifications, and
in laser ablation of polymers.

INTRODUCTION

Structures that develop on solid or liquid surfaces under the action of
laser light can be classified into *coherent* structures and *non-coherent*
structures. Coherent structures such as the so-called ripples, are *directly*
related to the coherence, the wavelength, and the polarization of the laser
light. For non-coherent structures a direct relation to laser parameters is
absent [1].
    The ranges where different types of coherent and non-coherent structures
are observed after UV-laser irradiation of PET (polyethylene-terephthalate)
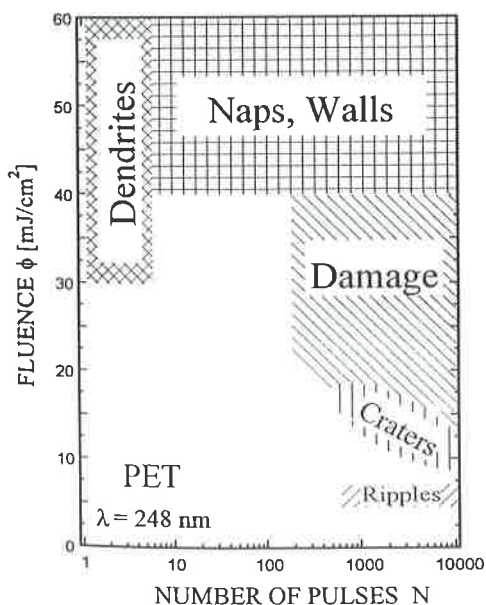are shown in Fig. 1.

Figure 1: Coherent (ripples) and non-coherent structures observed on PET after KrF-laser irradiation. The threshold fluence for ablation is ϕ_{th}(PET,248nm) $\approx$ 40 mJ/cm^2.

INSTABILITIES IN DIRECT WRITING

Non-coherent structures have been observed in different LCVD systems during pyrolytic direct writing. The oscillations shown in Fig.2a are neither related to the wavelength and polarization of the laser light nor to latent heat effects. Their period, Λ, has been found to increase with laser power, scanning velocity, the size of focus, and the pressure of the reactant gas. In the $WCl_6 + H_2 + (O_2)$ system, the oscillating behavior is closely related to changes in absorbed laser power due to changes in surface absorptivity. If the absorptivity increases with increasing temperature, there is a positive feedback which results in an increase in deposition rate. However, the increase in cross section of the stripe increases the heat loss due to conduction along the stripe, and the temperature drops again. Oscillations occur if in some temperature interval a sufficiently steep increase in absorptivity exists. This increase may be due to changes in surface chemistry and/or morphology.

The theoretical analysis of this phenomenon is based on the fact that the heat conductivity of the deposit, κ_D, is much higher than that of the substrate, κ_S, i.e. $\kappa^* = \kappa_D/\kappa_S \gg 1$. In this case, the heat flux is directed mainly along the metal line and then gradually dissipates into the substrate. This allows to treat the problem in one dimension and to calculate the temperature distribution for the given parameters of the line. From the balance between the deposition rate and material removal from the reaction zone due to scanning one can derive simplified equations for the evolution of the height, h, of the stripe and the temperature T_c near the position of the laser beam [3]

$$\frac{dT_c}{dt} \approx k_T \left[T_{c\ eq}(h, r_D) - T_c \right] \tag{1}$$

$$\frac{dh}{dt} \approx W(T_c) - v_s \frac{h}{r_D} \tag{2}$$

Here $k_T \approx D/\kappa^* r_D h$ is the temperature relaxation rate. k_T is much higher than the typical rate which determines changes in h. D is the thermal diffusivity. The first term in (2) describes the (Arrhenius) reaction rate and the second term material removal due to scanning with velocity v_s. The quasi-equilibrium temperature, $T_{c\ eq}$, may be calculated from the *stationary* heat equation. For high powers, $r_D \gg w_o$ and one obtains the transcendental equation [3,4]

$$\Delta T_{c\ eq} = T_c - T_o \approx \frac{P\ A(T_{c\ eq})}{4\ [\kappa_s \kappa_D r_D h]^{1/2}} \left[1 + \exp \left[-2 \left[\frac{r_D}{h\ \kappa^*} \right]^{1/2} \right] \right] \tag{3}$$

r_D should be determined from the condition that the temperature at the edge of the stripe is equal to the threshold temperature for deposition, T_{th}
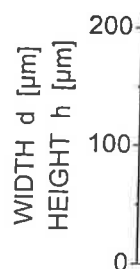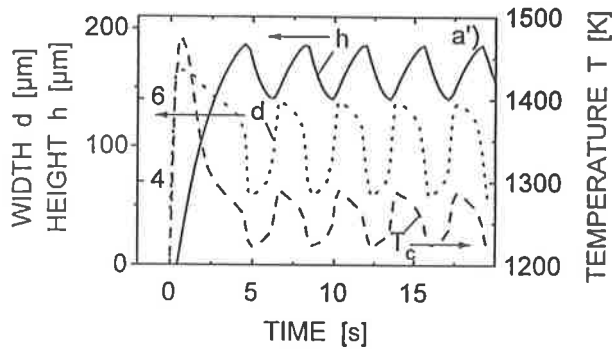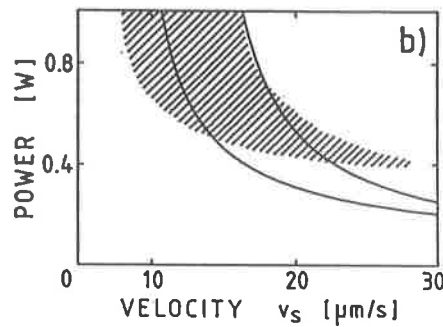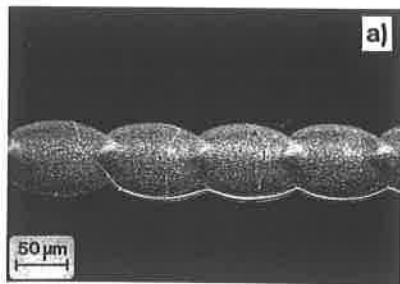
Figure 2: Periodic structure observed for a W line deposited from 1.1 mbar WCl$_6$ + 50 mbar H$_2$ + 15 μbar O$_2$ by 515 nm cw-Ar$^+$-laser direct writing (2w$_o$ = 15 μm) a) P = 650 mW, v$_s$ = 15 μm/s [2]. a') Calculated time-dependent behavior of the height h (full curve, inner scale on left axis), and width d = 2r$_D$ of stripes (dotted curve, outer scale on left axis) and the center temperature T$_c$ (dashed curve) [3]. b) The shaded area indicates the range of laser powers and scanning velocities where oscillations have been observed. The full curves have been calculated [4].

$$r_D = \kappa^* \, h \, \mathrm{arccosh}^2 \left[\frac{\Delta T_{c \ eq}}{\Delta T_{th}} \right] \tag{4}$$

P is the laser power and A(T) the temperature-dependent absorptivity. The (relaxation) oscillations in (1) and (2) satisfactory describe the experimental results (Fig. 2a').

Detailed calculations demonstrate that oscillations occur only within certain parameter ranges - in agreement with the experiments (Fig.2b).

Discontinuous deposition and bistabilities

The first clear observation of discontinuous growth was made during pyrolytic direct writing of Si-lines. For low laser powers a uniform line with a height of, typically, a few μm is observed (Fig.3a lower part). When a
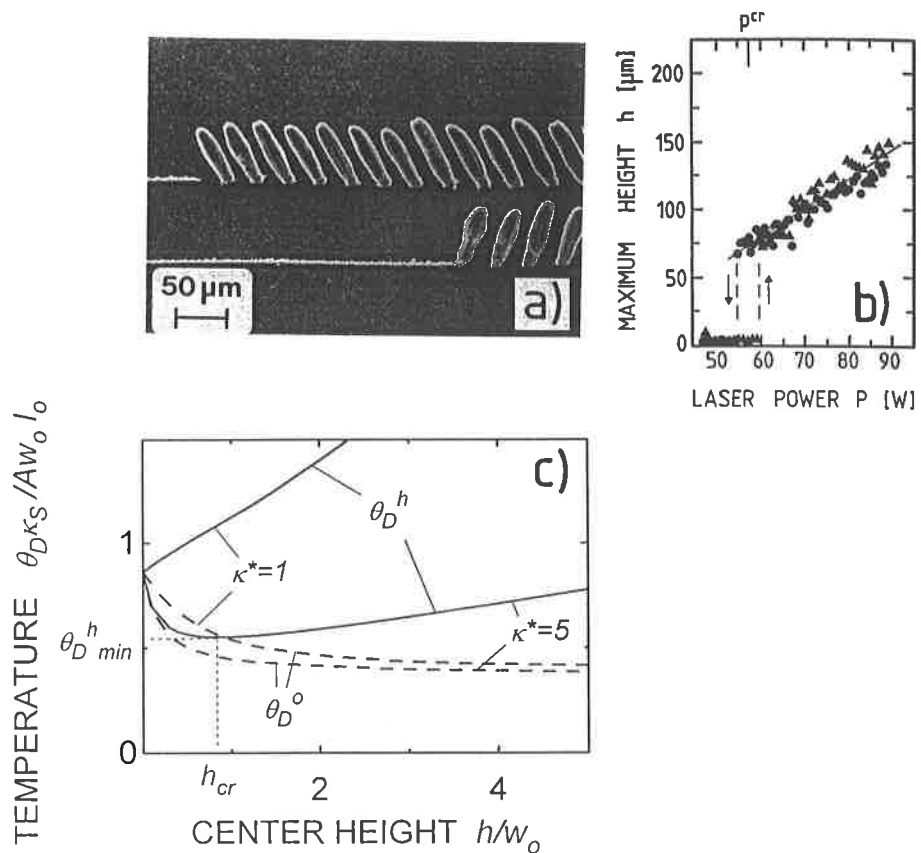
575

Figure 3: a) SEM picture of Si deposited by Ar^+-laser direct writing (λ = 515 nm, $2w_o$ = 3 μm, p(SiH$_4$) = 500 mbar). Lower trace: Constant scanning (v_s = 15 μm/s) from left to right with continuously *increasing* laser power from 53 mW to 63 mW. Upper trace: Scanning from right to left with *decreasing* laser power. b) Maximum height of deposits as a function of laser power at constant scanning velocity v_s = 15 μm/s. ▲ and ● refer to increasing and decreasing laser power [5]. c) Normalized dependence of θ_D^h (full curves) and θ_D^o (dashed curves) on the (normalized) height in the center, h/w_o . The deposit is a spot with parabolic shape with fixed radius r_D/w_o = 2, κ^* = 5 or 1 and $\alpha_D \rightarrow \infty$ (surface absorption). The critical height, h_{cr} , at which the temperature reaches a minimum, $\theta_{D\ min}^h$, is shown for κ^* = 5.

certain laser power is reached, the line becomes non-uniform. When the power is increased further, a discontinuous transition occurs. The deposit consists now of single, almost equidistant rods tilted into the scanning direction. The height of these rods increases continuously with laser power. Figure 3b) shows the height of deposits as a function of laser power. It becomes evident that there is a well-pronounced hysteresis (bistability). With increasing power the transition occurs at a *critical* power of $P^{cr} \approx 59$ mW, and with decreasing power at about 55 mW. P^{cr} increases with v_s . A similar behavior has been observed when the scanning velocity is varied at otherwise constant parameters.

Let us first consider the changes in temperature in the absence of scanning for $\kappa^* > 1$ and $\alpha_D \rightarrow \infty$. In the *initial* phase of growth the influence of the deposit can be ignored and the (stationary) linearized center temperature rise, θ_D^h , induced at the surface of the deposit by a Gaussian laser beam can be approximated by

$$\theta_D^h \approx \theta_D^o = \frac{\pi^{1/2}}{2} \frac{A\, I_o w_o}{\kappa_s} \tag{5}$$

where θ_D^o is the temperature at the interface between the substrate and the deposit. When a thin relatively wide spot with radius $r_D \approx 2\text{-}3\ w_o$ is formed, the temperature decreases because of *lateral* heat spreading and the growth in r_D slows down with respect to the growth in h. If $\kappa^* \gg 1$, θ_D^h decreases with increasing h up to a certain value, h_{cr} , where

$$\theta_{D\ min}^h \approx \theta_D^o \approx \frac{\pi\, A\, I_o w_o^2}{4\, \kappa_s\, r_D} \tag{6}$$

Subsequently, θ_D^h increases because a temperature gradient builds up in *vertical* direction. With thermally *thick* deposits and $h/w_o \gg h_{cr}/w_o$ we can use the approximation

$$\theta_D^h \approx \theta_D^o\ [\ 1 + \delta\ \frac{h}{\kappa^*\, r_D}\ ] \tag{7}$$

where θ_D^o is given by (6). δ depends on the shape of the deposit and it is of the order of unity. The calculated behavior of θ_D^h with h/w_o is shown in Fig. 3c for $\kappa^* = 1$ and 5 by the full curves. The temperature at the substrate-deposit interface, θ_D^o , *always* decreases (dashed curves). With $\kappa^* \leq 1$ the temperature θ_D^h increases for all values of h. With $\kappa^* > 1$ the minimal temperature $\theta_{D\ min}^h$ is reached with $h \approx r_D$. If $h_{cr}/r_D > 1$, the growth rate at the tip of the spot strongly increases and a *rod* starts to grow towards the laser beam. The geometry of this rod can be estimated by assuming one-dimensinoal heat conduction.

This model holds qualitatively also if the substrate is scanned. With

thick stripes (h ≈ r_D) i.e. with high laser powers or low scanning velocities, a rod may start to grow. The growth of the rod ceases when the laser beam intensity in the tip becomes too low. Then, the laser beam reaches the substrate again and the process repeats.

When we consider the transition from a uniform *line* to a rod, h/r_D should exceed the critical ratio which corresponds to $\theta^h_{D\ min}$. In the opposite case (decreasing power or increasing scanning velocity) deposition will become continuous if for the power and laser-beam dwell time employed h < h_{cr} in Fig. 3c. The hysteresis observed in the experiments can be understood along these lines: Roughly speaking, the transition occurs at a certain center temperature which requires a higher laser power for the transition line to rod than vice versa (in this latter case the heat loss by conduction along the line is absent).

These considerations show, that it is impossible to produce uniform stripes with h/r_D > 1 by single-scan pyrolytic direct writing.
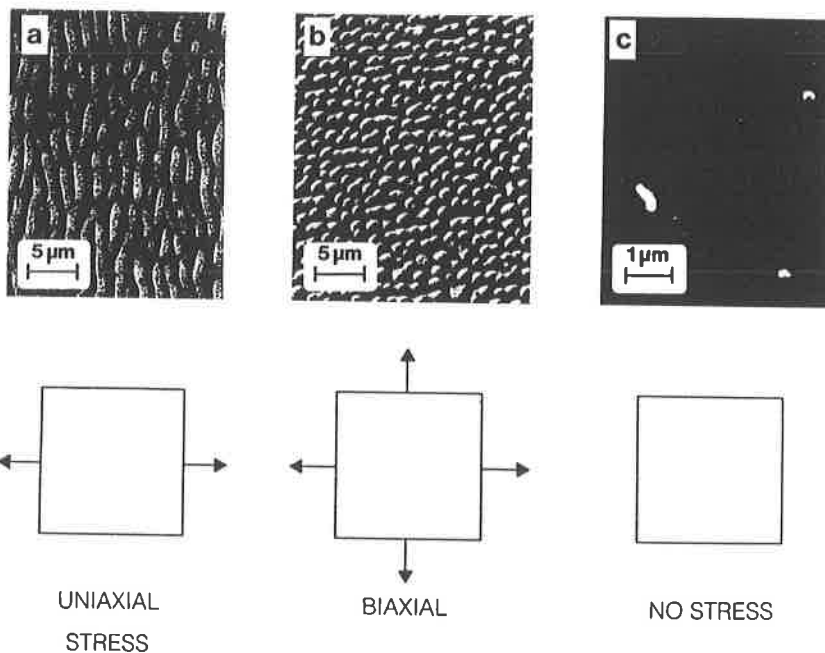
UNIAXIAL STRESS

BIAXIAL

NO STRESS

Figure 4: SEM micrographs of different types of structures observed on PI foils after ablation with KrF-laser radiation. a) Foil was uniaxially stretched before ablation (ϕ ≈ 136 mJ/cm², 30 pulses). b) Foil was biaxially stretched before ablation (ϕ ≈ 115 mJ/cm², 50 pulses). c) Annealed foil (ϕ ≈ 120 mJ/cm², 50 pulses) [6].

STRESS REL

Polymer
nap-type
stresses w
remains sm
perpendicu
walls or r
fluence.
A tenta
a stress-r
externally
Formation
energy dec

$$a \gtrsim a_c$$

where a is
σ the sur

The depth
related t
quasiperic
also expl
pulses.
ablation
both abla
structure
of the st
random di
the avera

DENDRITIC

Single
(Fig. 6a).
0.1 µm.
suppresse
dendrites
The growt

shows a

S

Figure 5
craze fo
field.

STRESS RELATED INSTABILITIES

Polymer surfaces ablated with UV-laser light frequently show wall- or nap-type structures (Figs.4). These structures are related to internal stresses within the polymer foil. The surface of annealed (unstretched) foils remains smooth. Naps seem to be formed by "superposition" of walls aligned perpendicularly to the respective stresses. The average distance between walls or naps increases with both the number of laser pulses and the laser fluence.

A tentative explanation for the formation of these structures is based on a stress-release model. Here, craze formation is considered to be due to an externally applied or frozen-in stress, S, parallel to the surface (Fig.5). Formation of a craze significantly changes the stress field. The overall energy decreases after craze formation if

$$a \geq a_c = \frac{2 \, Y \, \sigma}{\pi \, [1 - \mu^2] \, S^2} \tag{8}$$

where a is the depth of the craze, Y Young's modulus, μ the Poisson ratio and σ the surface tension. For polymers, we find as "average" value $a_c \approx 1 \, \mu$m.

The depth of the craze, which determines the volume of stress relaxation, is related to the thickness of the laser-heated surface layer. Thus, a quasiperiodic surface structure with a mean period $\Lambda \approx 2a$ develops. The model also explains, qualitatively, the increase in Λ with the number of laser pulses. Irradiation of a quasiperiodic structure leads to preferential ablation of top-layers where the stress fields are relaxed. At the bottom both ablation and further extension of the craze increase the depth of the structure. Simultaneously, the relaxed volume increases and the stabilization of the structure by the stress field becomes lost. Naps or walls drop over in random directions so that, for example, a new nap is formed out of two. Thus, the average period increases.

DENDRITIC STRUCTURES

Single-pulse UV-laser irradiation of PET induces the growth of dendrites (Fig.6a). KrF-laser light amorphizes the PET surface within a depth $\ell_\alpha \approx$ 0.1 μm. This layer recrystallizes, in part. Dendrite formation can be suppressed by coating the surface with a thin metal layer. The growth of dendrites starts at different nucleation centers within the irradiated area. The growth rate $G = \ell_m/t_g$ (ℓ_m = length of dendrite arms, t_g = time of growth) shows a maximum near the glass temperature, T_G, as shown in Fig. 6b.
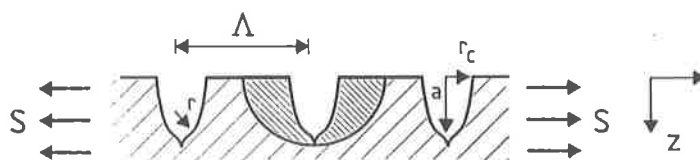

Figure 5: Schematic picture of quasiperiodic structures originating from craze formation in materials with frozen-in or externally applied stress field.
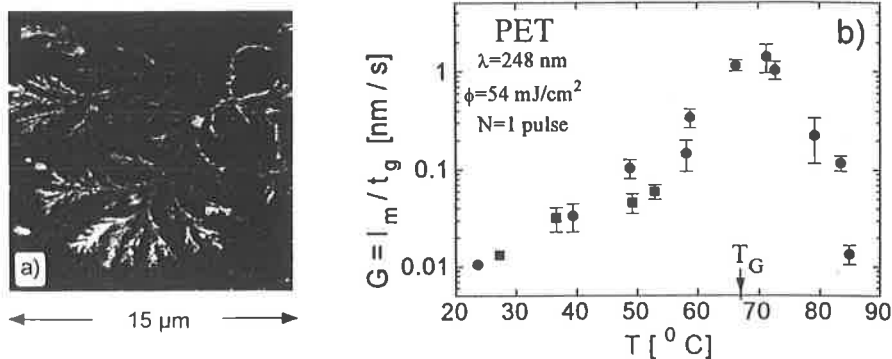
Figure 6: Dendritic growth on PET after single-pulse KrF-laser irradiation in vacuum. a) Atomic force microscope (AFM) picture of dendrite ($\phi = 41$ mJ/cm^2). Such dendrites are elevated above the surface by, typically, 5 to 30 nm and extended into the surface by about the same amount [7]. b) Growth rate $G = l_m/t_g$ of surface dendrites on PET-surfaces after irradiation with a single KrF-laser pulse of $\phi \approx 54$ mJ/cm^2. ■ after growth for 24 h in vacuum; ● after 2-24 h in 1 bar nitrogen atmosphere.

Dendrite formation may be related to the observation that the adhesion of metal films evaporated onto foils preirradiated with UV light is increased with respect to non-irradiated foils by up to more than a factor of ten [8].

REFERENCES

1. D. Bäuerle, Laser Processing and Chemistry, Springer, Berlin 1996;
D. Bäuerle, Chemical Processing with Lasers, Springer Series in Materials Science 1, Springer, Berlin 1986.
2. P.B. Kargl, R. Kullmer and D. Bäuerle, Appl.Phys. A 57, 175 (1993).
3. N. Arnold, P.B. Kargl, R. Kullmer and D. Bäuerle, Appl.Phys. A 61, 347 (1995).
4. N. Arnold, P.B. Kargl and D. Bäuerle, Appl.Surf.Sci. 86, 457 (1995).
5. P.B. Kargl, R. Kullmer and D. Bäuerle, Appl.Phys. A 57, 577 (1993).
6. E. Arenholz, M. Wagner, J. Heitz and D. Bäuerle, Appl.Phys. A 55, 119 (1992).
7. J. Heitz, E. Arenholz, D. Bäuerle, and K. Schilcher, Appl. Surf. Sci. 81, 103 (1994).
8. A. Hagemeyer, H. Hibst, J. Heitz and D. Bäuerle, J. Adhesion Sci. Technol. 8, 29 (1994).